

4

DTIC FILE COPY

AD-A205 263

OFFICE OF NAVAL RESEARCH

CONTRACT NO. N00014-86-K-0772

TECHNICAL REPORT NO. 34

The Effect of Hot Drawing on the Properties of Thermotropic Polymer Fibers

by

A. T. DiBenedetto, L. Nicolais, E. Amendola, C. Carfagna, and M. R. Nobile

Liquid Crystalline Polymer Research Center
University of Connecticut
Storrs, CT 06269-3136

Prepared for Publication
in
Polymer Engineering and Science

February 27, 1989

DTIC
SELECTED
S 2 MAR 1989 D
E

REPRODUCTION IN WHOLE OR IN PART IS PERMITTED FOR ANY PURPOSE OF THE UNITED STATES GOVERNMENT.

THIS DOCUMENT HAS BEEN APPROVED FOR PUBLIC RELEASE AND SALE; ITS DISTRIBUTION IS UNLIMITED.

89 3 01 129

REPORT DOCUMENTATION PAGE

| | | | | | | |
|---|-------|---|---|--|----------------------------------|-----------------------------|
| 1a REPORT SECURITY CLASSIFICATION Unclassified | | | 1b RESTRICTIVE MARKINGS None | | | |
| 2a SECURITY CLASSIFICATION AUTHORITY | | | 3 DISTRIBUTION/AVAILABILITY OF REPORT Approved for Public Release, Distribution Unlimited | | | |
| 2b DECLASSIFICATION/DOWNGRADING SCHEDULE | | | 5. MONITORING ORGANIZATION REPORT NUMBER(S) | | | |
| 4 PERFORMING ORGANIZATION REPORT NUMBER(S) Technical Report No. 34 | | | 7a NAME OF MONITORING ORGANIZATION Office of Naval Research | | | |
| 6a. NAME OF PERFORMING ORGANIZATION University of Connecticut | | 6b. OFFICE SYMBOL (if applicable) | | 7b ADDRESS (City, State, and ZIP Code) 800 North Quincy Avenue Arlington, VA 22217 | | |
| 6c. ADDRESS (City, State, and ZIP Code) Storrs, CT 06268 | | | 9 PROCUREMENT INSTRUMENT IDENTIFICATION NUMBER N00014-86-K-0772 | | | |
| 8a. NAME OF FUNDING/SPONSORING ORGANIZATION | | 8b OFFICE SYMBOL (if applicable) ONR | | 10 SOURCE OF FUNDING NUMBERS | | |
| 8c. ADDRESS (City, State, and ZIP Code) 800 North Quincy Avenue Arlington, VA 22217 | | PROGRAM ELEMENT NO. | PROJECT NO. | TASK NO. | WORK UNIT ACCESSION NO. | |
| 11 TITLE (Include Security Classification) "The Effect of Hot Drawing on the Properties of Thermotropic Polymer Fibers" (Unclassified) | | | | | | |
| 12 PERSONAL AUTHOR(S) A.T. DiBenedetto, L. Nicolais, E. Amendola, C. Carfagna, and M.R. Nobile | | | | | | |
| 13a TYPE OF REPORT Interim Technical | | 13b TIME COVERED FROM _____ TO 2/24/89 | | 14 DATE OF REPORT (Year, Month, Day) 1989-02-27 | | 15. PAGE COUNT 45 |
| 16 SUPPLEMENTARY NOTATION Prepared for publication in <u>Polymer Engineering and Science</u>, <u>29</u>, Mid-February, 1989 (LCPRC Publication No. 89-3) | | | | | | |
| 17 COSATI CODES | | | 18. SUBJECT TERMS (Continue on reverse if necessary and identify by block number) | | | |
| FIELD | GROUP | SUB-GROUP | → Liquid Crystal Polymers. (JES) | | | |
| | | | | | | |
| 19 ABSTRACT (Continue on reverse if necessary and identify by block number) <p>Thermotropic liquid crystal polymers have been modeled as an array of highly ordered polyhedric nematic domains immersed in a less-ordered, nearly isotropic matrix. A function has been defined that expresses the elastic moduli of drawn fibers as a function of orientation and geometry of the nematic domains. When such a material is hot drawn in extension, the domains orient and elongate to produce an orthotropic fibrous phase. Equations are proposed to relate the elastic moduli of the fibers to the draw ratio and the extrusion conditions. Upon annealing of the hot drawn fibers, shrinkage occurs. It is proposed that the shrinkage is the result of a physical transformation from the fibrous state back to the nematic domain structure present before extrusion and drawing. The Avrami equation is used to describe the nucleation and growth processes controlling the shrinkage at constant annealing temperature. The model is shown to correlate experimental data on the elastic properties and the shrinkage of hot drawn PET/PHB60 liquid crystal polymer with the processing conditions.</p> | | | | | | |
| 20 DISTRIBUTION/AVAILABILITY OF ABSTRACT <input checked="" type="checkbox"/> UNCLASSIFIED/UNLIMITED <input type="checkbox"/> SAME AS RPT <input type="checkbox"/> DTIC USERS | | | 21. ABSTRACT SECURITY CLASSIFICATION Unclassified | | | |
| 22a NAME OF RESPONSIBLE INDIVIDUAL Dr. Kenneth J. Wynne | | | 22b TELEPHONE (Include Area Code) (202) 696-4410 | | 22c. OFFICE SYMBOL ONR | |

| | |
|--------------------|-------------------------------------|
| Accession For | |
| NTIS GFA&I | <input checked="" type="checkbox"/> |
| DTIC TAB | <input type="checkbox"/> |
| Unannounced | <input type="checkbox"/> |
| Justification | |
| By _____ | |
| Distribution/ | |
| Availability Codes | |
| Dist | Avail and/or Special |
| A-1 | |

THE EFFECT OF HOT DRAWING ON THE PROPERTIES
OF
THERMOTROPIC POLYMER FIBERS



A.T. DIBENEDETTO
UNIVERSITY OF CONNECTICUT
DEPT. OF CHEMICAL ENGINEERING
INSTITUTE OF MATERIALS SCIENCE
STORRS, CT.

L. NICOLAIS, E. AMENDOLA, C. CARFAGNA, M.R. NOBILE
UNIVERSITY OF NAPLES
DEPARTMENT OF MATERIALS AND PRODUCTION ENGINEERING
NAPLES, ITALY

ABSTRACT

Thermotropic liquid crystal polymers have been modeled as an array of highly ordered polyhedric nematic domains immersed in a less ordered, nearly isotropic matrix. A function has been defined which expresses the elastic moduli of drawn fibers as a function of orientation and geometry of the nematic domains. When such a material is hot drawn in extension the domains orient and elongate to produce an orthotropic fibrous phase. Equations are proposed to relate the elastic moduli of the fibers to the draw ratio and the extrusion conditions. Upon annealing the hot drawn fibers, shrinkage occurs. It is proposed that the shrinkage is the result of a physical transformation from the fibrous state back to the nematic domain structure present before extrusion and drawing. The Avrami equation is used to describe the nucleation and growth processes controlling the shrinkage at constant annealing temperature. The model is shown to correlate experimental data on the elastic properties and the shrinkage of hot drawn PET/PHB60 liquid crystal polymer with the processing conditions.

THE EFFECT OF HOT DRAWING ON THE PROPERTIES
OF
THERMOTROPIC POLYMER FIBERS

A. T. DIBENEDETTO
UNIVERSITY OF CONNECTICUT
DEPT. OF CHEMICAL ENGINEERING
INSTITUTE OF MATERIALS SCIENCE
STORRS, CT.

L. NICOLAIS, E. AMENDOLA, C. CARFAGNA, M.R. NOBILE
UNIVERSITY OF NAPLES
DEPARTMENT OF MATERIALS & PRODUCTION ENGINEERING
NAPLES, ITALY

INTRODUCTION

Thermotropic polymers produce a high degree of molecular orientation during processing in the melt state and are able to maintain this orientation during solidification. Relatively rigid backbone molecules produce anisotropic or orthotropic structures capable of being formed into high stiffness and strength fibers. Since they can be processed in conventional processing equipment they are prime candidates for reinforcement of conventional thermoplastic and thermoset polymers (1-6). Over the past few years a number of research groups have studied the processing characteristics of thermotropic polyester and copolyester fibers. McFarlane et.al.(1), Ide and Ophir (2), Ide and Chung (3), Calundann and Jaffe (4), Baird and Wilkes (5) and Zhou et.al. (6) have all examined the effects of polymer composition and shear and extensional flow on the mechanical properties of extruded and drawn thermotropic polymers.

When the nematic liquid crystal phase is extruded, either alone or in a blend, it will undergo both shear and elongational flow. The orientation and texture upon exiting the extruder will be complex because

of the variation of flow field within the extruder and at the die exit. Within the extruder the orientation of the nematic phase will vary from highly oriented at the walls to much less oriented at the center. The variation in structure, resulting in a skin-core effect, has been studied by a number of investigators (2-5). When the melt is hot drawn in an extensional flow field the nematic domains are oriented in the direction of extension and appear to be drawn into an oriented fibrous form with a high length-to-diameter ratio. Since the relaxation of the fibers and reversion back to a disoriented isotropic state is negligible in the solid state, they provide an attractive alternative to glass, graphite and other more traditional reinforcements. It has also been shown that liquid crystal polymers containing chemically disordered chains can undergo a phase transition from a nematic to an isotropic state over a broad range of temperature, which results in the formation of a two-phase material (7-8). Based on the general appearance of the highly drawn fibers, we propose that upon exiting the extruder the thermotropic melt can be considered an array of polyhedral nematic domains interconnected through nearly isotropic boundaries of less ordered material. When an extensional stress is imposed, the material behaves much like an elastic network during draw, and is capable of relieving internal stresses after drawing by relative movement of the deformed nematic regions through shearing of the oriented, but weak, matrix boundaries. We will describe the elastic properties of hot drawn thermotropic fibers as a function of draw ratio, temperature and extrusion conditions. We will also describe the relaxation behavior of these materials as a function of annealing time and temperature. The model will be compared to data on drawn PET/PHB60 thermotropic polymer fibers.

MORPHOLOGICAL STUDIES

The following morphological analysis of the nematic structure of a PET/PHB60 liquid crystal polymer (LCP) is the basis for the mathematical modelling of the LCP hot drawing process. The nematic phase is assumed to be composed of highly oriented domains interconnected through boundaries of less ordered material. The orientation, size and shape of the nematic domains are sensitive to temperature, pressure, shear and elongational stresses and electromagnetic fields. The effects of time and temperature on the structure of PET/PHB60 are shown in Figure 1. When a thin film of the LCP is observed at 220°C between cross polarizers a faint texture is evident and is the result of the slight shear stresses imposed on the material while preparing the sample for microscopy. No macroscopic orientation is detectable when rotating both the cross polarizers, indicating that the nematic domains are randomly oriented throughout the film. As the temperature is increased, the fine structure of the submicron domains transforms to a much coarser texture. For example, after 25 minutes of annealing at 260°C the domains appear to agglomerate into well-defined, macroscopically oriented domains of up to 10 to 15 μm . The black spots in Figure 1b are highly anisotropic zones, as clearly shown by rotating both polarizers. The black areas turn light upon rotation of the polarizers, indicating that the molecules in the domains are oriented perpendicular to the analyzers. One can clearly see a distribution of domain sizes and, with time, the smaller domains evolving into larger, more stable zones. (We will show later that hot drawing of the material at this temperature results in a fibrous structure with a broad distribution of fiber diameters.) As the temperature is increased further to 300°C

and held for 10 minutes (Figure 1c), black brush-like areas appear, which are well-known characteristics of a nematic phase (7-9). The brush lines meet at disinclination points still present in the structure. The boundaries between the domains are now much broader, and large portions of highly oriented material are clearly detectable.

When the material is extruded and hot-drawn at 260°C, a highly oriented fibrous structure results (10). In Figure 2a a portion of an LCP fiber drawn at a draw ratio of 250 is shown before and after rotating the polarizers by 45°. The texture of the specimen is clearly fibrous, and both long and short fibers can be identified (Figure 2a). Rotating the polarizers 45°, one can see boundaries between the oriented fibers in which the molecules are oriented at angles other than the draw axis (Figure 2b). Both scanning electron micrographs (Figure 3a) and optical micrographs (Figure 3b) of fracture surfaces of the drawn fibers confirm the presence of a fibrous texture. As can be seen the highly drawn fibers appear to have two distinct characteristics. There are fibrous elements with diameters of the order of a few to 10 microns that consist of bundles of very fine filaments in the sub-micron region. These bundles appear to be held together in much the same fashion as in fiber reinforced composites, thus forming a high strength composite filament. Upon annealing the drawn fibers, shrinkage accompanied by structural changes occurs. Ellipsoidal shaped nuclei develop around well-defined points in the fiber structure. These are possibly disinclination points still present in the drawn material. These nuclei appear to evolve into

three-dimensional symmetric nematic domains, randomly oriented throughout the fibrous structure. Figure 4a shows the first stage of the shrinkage phenomenon. Ellipsoidal particles are detectable at 230°C after 15 minutes annealing. Spherical particles are formed if the temperature is raised to 270°C (Figure 4b), and with a further increase in the temperature the spherical domains appear to agglomerate as a consequence of the low viscosity of the fluid phase. The fluid polymer quickly spreads over the glass surface of the cover slide and the resulting structure, being determined primarily by the interfacial tension with the glass substrate, is no longer representative of the original fiber.

On the basis of these observations we will propose an analytic "composites" model to characterize the properties of drawn LCP fibers and will use an Avrami-type nucleation and growth model to describe the kinetics of nucleation and growth of included nematic domains in the fibrous structure during annealing.

THEORY

1. Characterization of the Thermotropic Phase Using an Orientation Function

Immediately upon exiting an extruder the partially oriented nematic phase is assumed to consist of highly ordered domains more or less randomly dispersed in a less-ordered transition region, as shown schematically in Figure 5. The ordered domains are assumed to be polyhedral, occupy a volume fraction X_N , independent of the processing conditions, and have an orientation relative to the draw axis characterized by an orientation function S_N . The less-ordered zones surround the domains, are assumed to have very low shear and transverse moduli and have an orientation characterized by an orientation function

S_A . The overall molecular orientation of the thermotropic material is the volumetric average of the orientations of the two regions and is characterized by S_F . We will propose a composite model to describe the modulus of this thermotropic phase as it deforms in the extensional stress field generated during hot drawing. In the absence of stress the highly ordered nematic zones would probably take on a nearly spheroidal shape, but in the shear and extensional fields within the extruder they are deformed into a complex shape which is probably not far from being ellipsoidal with the major axis oriented in the direction of flow. Because of a high degree of extension at the extruder walls the surfaces of the extrudate are highly oriented, while toward the center the orientation is more random. A common view of the structure of the thermotropic material at rest is that of randomly oriented micron or sub-micron size domains of highly ordered molecules surrounded by boundaries of lesser order. The domains elongate by slippage of the oriented molecules past one another since the shear moduli of both the oriented domains and the surrounding non-ordered material are low. The process is shown schematically in Figure 5. Under the extensional field the domains will rapidly orient and elongate in the direction of flow and the fiber will approach, in the limit of very high elongation, an assembly of cylindrically symmetric, orthotropic bundles of chains preferentially aligned in the direction of flow, akin to the aggregate model originally proposed by Ward (11,12). The overall molecular orientation of the domains can be characterized by a vector, called the director, which is a measure of the orientation relative to the draw axis. Before the start of flow these vectors are randomly distributed if no previous flow history is present. In the limit of very high draw ratio the vectors tend to line up in the direction of draw.

Let us assume that immediately upon exiting the extruder the nematic domains of the thermotropic material can be characterized by average director angles, φ_i . An orientation parameter, S_N can be defined in terms of the average values of the $\cos^2 \varphi_i$ of all vectors which characterize the directions of the molecules which make up the domains. (The longitudinal direction is defined as the direction of draw.) The orientation function S_N is defined as follows:

$$S_N = (1/2) * (3 \langle \cos^2 \varphi \rangle - 1) \quad (1)$$

where:

$$\langle \cos^2 \varphi \rangle = \frac{\int_0^\pi g(\varphi) \cos^2 \varphi \sin \varphi \, d\varphi}{\int_0^\pi g(\varphi) \sin \varphi \, d\varphi} \quad (2)$$

where $g(\varphi)$ is an angular distribution function for the molecular vectors. For perfect orientation in the direction of flow, $\varphi = 0$ and $S_N = 1$. For perfect orientation perpendicular to the direction of flow, $\varphi = \pi/2$ and $S_N = -1/2$. For random orientation, $g(\varphi)$ is a constant and $S_N = 0$. If the boundaries that surround the nematic domains were perfectly isotropic, they could be represented by an orientation function $S_A = 0$.

2. Relation of the Orientation Functions to Processing Conditions.

When an extrudate is drawn at constant temperature and a draw ratio (DR) of greater than one there is an elongation of the nematic domains in the direction of flow under the influence of a uniform

extensional stress field, as shown schematically in Figures 5 and 6. Analysis of the surface zone is quite complex because of the rapidly changing temperature and state of stress. Analysis away from the surface, however, is less difficult because the temperature change is slow and a nearly uniaxial state of stress exists. Furthermore, during the drawing stage of the process the thermotropic melt will behave mechanically much like an elastic network in a state of uniaxial tension. Thus, let us imagine that the molecular vectors will behave as rigid rods rotating in a homogeneous medium exposed to a uniaxial extensional stress (Figure 7). In such a field of stress a rigid rod aligns itself in the direction of the tension. If the rod enters the extensional stress field at an angle to the applied tension it will orient continuously and its final angular position depends on the draw ratio imposed. It has been shown (13) that for a thin sheet or a cylindrically symmetric fiber the relation between the final angle of orientation and the initial angle is given by:

$$\tan(\varphi_f) = \tan(\varphi_o) / DR^{1.5} \quad (3)$$

Since one ordinarily starts at the exit of the extruder with a material possessing a distribution of liquid crystal domain orientation angles, the final material will have a distribution of LC fiber orientation angles described by Equation(2). One can relate the final orientation function to the initial distribution and the draw ratio DR in the following manner:

$$\varphi_f = \text{TAN}^{-1}(\text{TAN} \varphi_o / DR^{1.5}) \quad (4)$$

$$\text{COS}^2 \varphi_f = DR^3 / (\text{TAN}^2 \varphi_o + DR^3) \quad (5)$$

$$\langle \cos^2 \varphi_f \rangle = \frac{\int_0^\pi g(\theta) \cos^2 \theta \sin \theta d\theta}{\int_0^\pi g(\theta) \sin \theta d\theta} \quad (6)$$

where: $\theta = \varphi_f$, and $g(\theta)$ is the orientational distribution function expressed in terms of the initial distribution of orientation angles and the imposed draw ratio. Thus, from data on the orientation distribution at the exit of the extruder, $g(\varphi_0)$, one can calculate the final orientation function for the nematic domains, $(S_N)_f$, as a function of draw ratio.

A simple approximation of the integrals can be obtained by replacing the true initial angular distribution with an "average" constant value $\bar{\varphi}_0$. We define this average value in the following manner:

$$\cos \bar{\varphi}_0 = \langle \cos^2 \varphi_0 \rangle^{1/2} = [(2S_{N0} + 1)/3]^{1/2} \quad (7)$$

Substitution of equation (7) into the previous equations generates equation (8):

$$(S_N)_f = \frac{(2S_{N0} + 1)(DR)^3 - (1 - S_{N0})}{(2S_{N0} + 1)(DR)^3 + 2(1 - S_{N0})} \quad (8)$$

Equation (8) expresses the effect of draw ratio on the orientation function for the nematic domains.

We assume that in the absence of external stresses the nematic domains are randomly oriented polyhedra with an average aspect ratio (i.e., length to diameter ratio) of one. In the presence of a stress field the domains simultaneously rotate and elongate. Figure 5 shows that $(S_N)_f$ will range from 0 when $(l/d)=1$ and the domains are randomly oriented, to 1.00 when $(l/d) \rightarrow \infty$ and they are perfectly oriented along the axis of draw. As the domains rotate and translate in the extensional field, the length-to-diameter ratio increases as a function of the draw ratio. If the directors rotate as rigid rods, $(S_N)_f$ will approach 1.00 at a relatively low draw ratio. If the oriented domains are easily deformable and can be drawn at constant volume, one may assume that the major axes (l) will vary directly with the draw ratio. Since $l_f * d_f^2 = l_o * d_o^2$, the aspect ratio of the ellipsoid, (l/d) , will vary with $(DR)^{1.5}$. On the other hand, if the nematic domains are rigid and thus non-deformable, their shape will be independent of draw ratio and the aspect ratio remains constant during the drawing process. We will assume that at constant temperature the final aspect ratio of the nematic domains, $(l/d)_f$, varies as a power law function of the draw ratio:

$$(l/d)_f = (l/d)_o * (DR)^{3n/2} \quad (9)$$

where (n) is equal to zero for a nondeformable domain and equal to one for a readily deformable domain. The lower limit $n=0$ can occur both at low drawing temperature where the domains are too rigid to be deformed in the extensional stress field and at high drawing temperatures where the shear modulus (or viscosity) of the disordered boundaries is too low to transmit the necessary extensional stress to the immersed nematic domains.

Equations (8) and (9) thus relate the orientation and deformation of the nematic domains to the extrusion and hot drawing conditions. The disordered material in the boundaries must also deform and orient, but it is not as easily represented by rigid rod rotation and probably relaxes back to a random orientation much more readily at process conditions. We will assume that the boundary material remains nearly isotropic at processing temperatures, and if biaxial orientation appears likely its structure may be assumed to be orthotropic.

3. Relation of Elastic Moduli of the Fiber to Processing Conditions.

The thermotropic material is visualized as a distribution of polyhedral liquid crystal domains embedded in a less ordered matrix. Upon hot-drawing, the nematic domains are oriented in the direction of draw. Although the matrix (boundaries) can also be oriented, it is assumed that it has properties more akin to those of an ordinary amorphous polymer so that rapid relaxation will maintain a nearly isotropic mass. We then use the well-known Halpin-Tsai equation to calculate the moduli of the "composite" thermotropic phase (14). For the longitudinal and transverse moduli of the drawn fiber in which the nematic liquid crystal domains are perfectly oriented in the direction of extension, (i.e., $S_N=1$), we use:

$$\frac{(E_J)_F}{E_{AJ}} = \frac{1 + ABX_N}{1 - BX_N} \quad (10)$$

where J=L (Longitudinal) or T (Transverse), and:

$$B = \frac{(E_N/E_A)_J - 1}{(E_N/E_A)_J + A} \quad (11)$$

The quantity A is equal to $2*(1/d)$ for the longitudinal direction (J=L), where $(1/d)$ is the length to diameter ratio of the polyhedral liquid crystal domains, and $A=2$ for the transverse direction (J=T). The quantity X_N is the volume fraction of the oriented liquid crystalline domains of the thermotropic material, and the E_{AJ} and E_{NJ} are the longitudinal and transverse moduli of the matrix (boundaries) and liquid crystalline domains respectively. Wide angle X-ray scattering (WAXS) data on highly oriented fibers can be used to estimate the volume fraction of the oriented liquid crystalline domains. The measured value of the molecular director of the fiber is the average of the molecular vectors in both the nematic domains and the less-ordered boundaries. If the molecular director is S_N for the nematic domains and $S_A=0$ for the disordered matrix boundaries, one can express the net director S_F as:

$$S_F = X_N * S_N + (1 - X_N) * S_A = X_N * S_N \quad (12)$$

For example, we have found that the highly drawn fibers used in this study appear to approach a maximum value of $(S_F)_f = 0.81$ to 0.83 (as measured by WAXS). At a draw ratio of 300 (the maximum experimental value) S_N should be virtually equal to one, so that X_N should be approximately equal to 0.81 to 0.83 .

The longitudinal modulus of the fiber, $(E_L)_F$, can then be expressed as a function of the orientation and distortion of the nematic domains. When the nematic zones are perfectly oriented the fiber may be treated as an orthotropic material and its longitudinal and transverse moduli can be calculated with reasonable accuracy using equations 10 and 11. When the nematic zones are distributed about the draw axis, ($S_N < 1.00$), a weighting function has to be defined in order to account for the decrease in stiffness associated with the off-axis fiber elements. For continuous fiber elements:

$$(E_L)_F = E_L * X_N * f + E_A * (1 - X_N) \quad (13)$$

where:

$$f = \frac{\int_0^\pi g(\varphi_f) d\varphi_f}{\int_0^\pi d\varphi_f} \quad (14)$$

The quantity $g(\varphi_f)$ is the orientation distribution function of the nematic domains. In the absence of sufficient information to calculate (f) and when the average orientation angle, $\bar{\varphi}_f$, is relatively small, an alternate approach to calculating the effective longitudinal modulus is to consider the fiber as an orthotropic body loaded at angle $\bar{\varphi}_f$ to the

longitudinal axis. The general expression for the angular dependence of the modulus is then:

$$\frac{1}{(E_L)_F} = \frac{\cos^4 \bar{\varphi}_f}{E_L} + \frac{\sin^4 \bar{\varphi}_f}{E_T} + \frac{1}{4} \left(\frac{1}{G_{LT}} - \frac{2\nu_{LT}}{E_L} \right) \sin^2 2\bar{\varphi}_f \quad (15)$$

where E_L , E_T and G_{LT} are the longitudinal, transverse and shear moduli of the fiber respectively, and ν_{LT} is the Poisson ratio. A satisfactory approximation to equation (15) has been proposed by Lees(15):

$$(E_L(\bar{\varphi}_f))_F = E_L * E_T / (E_L - (E_L - E_T) * \cos^4 \bar{\varphi}_f) \quad (16)$$

Equation (16) will produce values within 10 percent of those using equation (15) when $\bar{\varphi}_f$ is two degrees or less. Since in most practical situations a draw ratio of at least ten is required to produce a good fiber, the average orientation angle $\bar{\varphi}_f$ for the nematic domains will likely be less than two degrees and equation (16) should be adequate for estimating the longitudinal modulus. The modulus, $(E_L)_F$, calculated using equations (13) or (16) can be equated to the apparent longitudinal modulus deduced from changes in the meridional X-ray scattering as a function of tensile stress (12). Ward has shown that $(E_L)_F$ can be estimated from measurements of longitudinal and shear moduli on liquid crystals with known orientation. Equation (16) provides the relation between the longitudinal modulus and the average angle of orientation $\bar{\varphi}_f$. Calundann and Jaffe (4) have provided experimental data on the dependence of tensile modulus on the molecular orientation angle as determined by

wide angle X-ray diffraction. The results obtained in this work are not comparable with theirs since they reported the angular dependence of very highly oriented liquid crystal polymers ($S_F > 0.9$), while the polymers used in this study had a maximum value of $S_F = 0.83$. However, the decreases in $(E_L)_F$ with the changes in S_N were quite similar.

4. Relaxation During Annealing of Hot Drawn Thermotropic Fibers.

In supercooling the drawn fibers a highly distorted liquid crystal structure is frozen in. Upon annealing at a high enough temperature there will be a tendency for relief of the internal strain by a disorientation which results in a shrinkage of the fiber. We assume that the principal mechanism for strain relief will be a physical transformation from the cylindrically symmetric fibrous state ($S_F = 1$) to the original randomly oriented nematic domains which made up the liquid crystal melt ($S_F = 0$). Reformation occurs around point sources still present in the drawn fiber, each of which acts as a nucleation site. Using the kinetic theory developed for isothermal crystallization, one can obtain a general equation for the fraction of material $x(t)$ transformed isothermally at time t (16-17):

$$x(t) = x(\infty) * (1 - \exp(-kt^3/x(\infty))) \quad (17)$$

The parameter $x(\infty)$ is the maximum mass of material transformed at the annealing temperature and k is a growth rate constant.

The shrinkage of the fiber is caused primarily by the change in shape from the cylindrical geometry with the high (l/d) ratio to polyhedral domains with $(l/d) = 1$. If one neglects shrinkage of the untransformed mass, the linear shrinkage is given by:

$$R = l_f(t=0)/l_f(t) = (1/d)_f / (x(t) * (1/d)_f^{1/3} + (1-x(t)) * (1/d)_f) \quad (18)$$

We assume that the drawn fiber has a fixed number of potential nucleation sites around which micron-size domains can form. An increasing number of these sites will nucleate as the annealing temperature is raised, so that $x(00)$ increases with temperature (and perhaps draw ratio at constant temperature). Shrinkage data will be used to evaluate k and $x(00)$ as a function of temperature and draw ratio.

EXPERIMENTAL PROCEDURES

The thermotropic liquid crystal polymer (LCP) was supplied by Tennessee Eastman Company. It is the well-known copolyester (PET/PHB60) first synthesized by Jackson and Kuhfuss in 1976 and is composed of 40 mole percent polyethyleneterephthalate and 60 mole percent p-hydroxybenzoic acid. The transition temperatures of the polymers were measured with a Differential Scanning Calorimeter (DSC), Mettler TA 3000 System. The temperature range 0 to 500 °C was scanned at a rate of 10°C/min. The LCP fibers were spun in a CEAST Rheoscope 1000 capillary viscometer equipped with a melt spinning unit using a flat entry die with a diameter of 1 mm and a length-to-diameter ratio of 10. Fibers were extruded at a rate of 45 cm/min and a temperature of 260°C. Filaments were extruded into air at room temperature and collected on a take-up spool placed at a distance of 30 cm from the die exit. The take-up velocity was varied in order to obtain draw ratios (DR) ranging from 10 to 300. The true draw ratio was determined by measuring the final diameter of the fiber, d_f , by means of an optical microscope, and calculating $DR = d_f^2 / (1.0\text{mm})^2$.

The longitudinal modulus of the LCP fiber was determined by measuring the elastic component of the complex modulus in a Dynamic Mechanical Spectrometer (Dynastat) at room temperature and a frequency of 1.0 Hz, using ASTM D 3399 as a standard procedure. Shrinkage measurements over a range of annealing temperatures of 180 to 240°C were made on LCP fibers drawn at a DR of 60 and 25. The initial length was chosen as 3 mm. (Longer specimens gave a spiral-like deformation upon shrinkage, probably due to inhomogeneities in the samples.) The 3 mm specimens were submerged in a silicon oil, Wacker APS 200, in an aluminum crucible. The oil did not swell the fibers to any measurable extent. To avoid the sticking of the fibers to the aluminum crucible, a thin Teflon film was placed in the bottom. The temperature of the heating medium was controlled with a Mettler FP 84 hot stage, and the change of diameter as a function of annealing time was observed with an optical microscope. The average of 20 measurements at each temperature was recorded. The standard deviation of each set was generally of the order of 10 percent. Data were reported as $R = d_t^2/d_o^2$ versus time, where d_t is the fiber diameter at a given time and d_o is the initial diameter.

The morphology of the LCP fibers was observed by means of both a Scanning Electron Microscope (SEM), Stereoscan 100, and an optical microscope (OP) with cross polars, Nikon LABOPHOT, equipped with a LINKAM TMS 90 hot stage. Transverse sections of the fibers were obtained by fracturing the specimens in liquid nitrogen. Wide angle X-ray diffraction patterns were obtained with a Siemens AED Automatic Diffractometer with $\text{CuK}\alpha$ radiation at room temperature. The order parameter " S_F " was calculated using numerical methods. Because of the small dimensions of the drawn fibers, (about 100 μm diameter), exposure times of 8 to 24 hours were required.

DISCUSSION OF RESULTS

The PET/PHB60 liquid crystal polymers were extruded and then rapidly hot drawn at high draw ratios. A typical result for a fiber extruded at a temperature of 260°C is shown in Figure 8. One sees a rapid 20-fold increase of tensile modulus, reaching a plateau at about a draw ratio of 100. Equations 8 to 11 were used to correlate the tensile modulus with draw ratio. A value of $X_N=0.83$ was obtained from WAXS data of the highly drawn fiber. The transverse properties of the oriented fibers have a relatively minor effect on the longitudinal tensile modulus at high draw ratio ($DR>5$), but a substantial effect at low draw ratio where calculations using equation 16 are suspect. It appears, however, that a value of $E_T=0.5\text{GPa}$ for the transverse modulus of the oriented fiber provides an adequate fit of the modulus versus draw ratio at values of $DR>10$. Based on WAXS data, the initial value of the order parameter upon exiting the extruder was $S_F=0.12$, indicating a relatively low degree of order. We obtained a value for the modulus of the nematic domains, $E_L=55\text{GPa}$, from the limiting fiber modulus at very high draw ratio and then chose the best value of the distortion parameter $n=0.5$ to obtain a good fit over the whole range of draw ratio. As can be seen, the equations correlate well with the experimental data. Assuming that the drawing zone is isothermal, one can interpret the value $n=0.5$ as a measure of the resistance to distortion of the nematic domains at the drawing temperature of 260 °C. At a lower drawing temperature one would expect a greater resistance to deformation and thus a smaller reinforcing effect. As the temperature is raised one would expect (n) to increase toward one and then decrease very rapidly toward zero as the shear modulus (or

viscosity) of the disordered regions becomes too low to permit deformation of the nematic domains. Actually, however, the drawing temperature was not well controlled, so the measured value of (n) may not have absolute significance. It was found, however, that the acceptable draw temperature range was rather narrow.

Figures 9 and 10 show the shrinkage of the fibers as a function of time at constant annealing temperatures. As can be seen, the shrinkage is very rapid, reaching a plateau almost immediately. Only at the highest combined temperature and total shrinkage ($R > 3$ and $T > 240^{\circ}\text{C}$) do we observe a lag time greater than a few minutes in reaching the plateau. From Equation 17 we deduce that the growth rate constant (k) is large enough to allow the exponential term to decrease to zero within a minute or two of reaching the annealing temperature. A value of $k = 0.15 \text{ min}^{-3}$ at $T = 240^{\circ}\text{C}$ produces an appropriate lag time at that temperature. The maximum shrinkage at constant annealing temperature can be correlated with the Avrami parameter $x(\infty)$ as shown in Figure (11). Also shown is the temperature dependence of $x(\infty)$. Virtually no shrinkage (thus no transformation) occurs below 180°C , while maximum shrinkage (thus complete transformation) occurs at temperatures approaching 255°C (528°K). As can be seen, $x(\infty)$ appears to vary linearly with the inverse of absolute temperature of annealing. Experimentally, it was found that the drawn fibers appear to revert spontaneously to their original shape at annealing temperatures above 250°C , well below the onset of the liquid crystal - isotropic transformation temperature (shown in Figure 12), and within the range where the model predicts a very rapid change in shrinkage with increasing temperature. From equation 18 one finds that the shrinkage will increase with increasing draw ratio at constant $x(\infty)$, but not to the

extent shown in Figure 10. Thus it appears that $x(00)$ may be a function of draw ratio as well as temperature, which is not unreasonable.

CONCLUSIONS

Liquid crystal polymers with chemically disordered chains, such as the processable thermotropic copolyesters, have been modeled as an array of highly ordered polyhedral nematic domains immersed in a less-ordered, nearly isotropic matrix. A function has been defined which expresses the elastic moduli of drawn fibers as a function of orientation and geometry of the nematic domains. When such a material is hot drawn in extension, the domains orient and elongate to produce an orthotropic fibrous phase. Equations are proposed to relate the elastic moduli of the fibers to the draw ratio and the extrusion conditions. Upon annealing the hot drawn fibers, shrinkage occurs. It is proposed that the shrinkage is a result of a physical transformation from the fibrous state back to the nematic domain structure present before extrusion and drawing. The Avrami equation is used to describe the nucleation and growth processes controlling the shrinkage at constant annealing temperature. The model is shown to correlate experimental data on the elastic properties and the shrinkage of hot drawn PET/PHB60 liquid crystal polymer with processing conditions.

ACKNOWLEDGEMENT

The authors wish to thank ENIRICERCHE, Milan, Italy, and the Liquid Crystalline Polymer Research Center at the University of Connecticut for support of this project.

REFERENCES

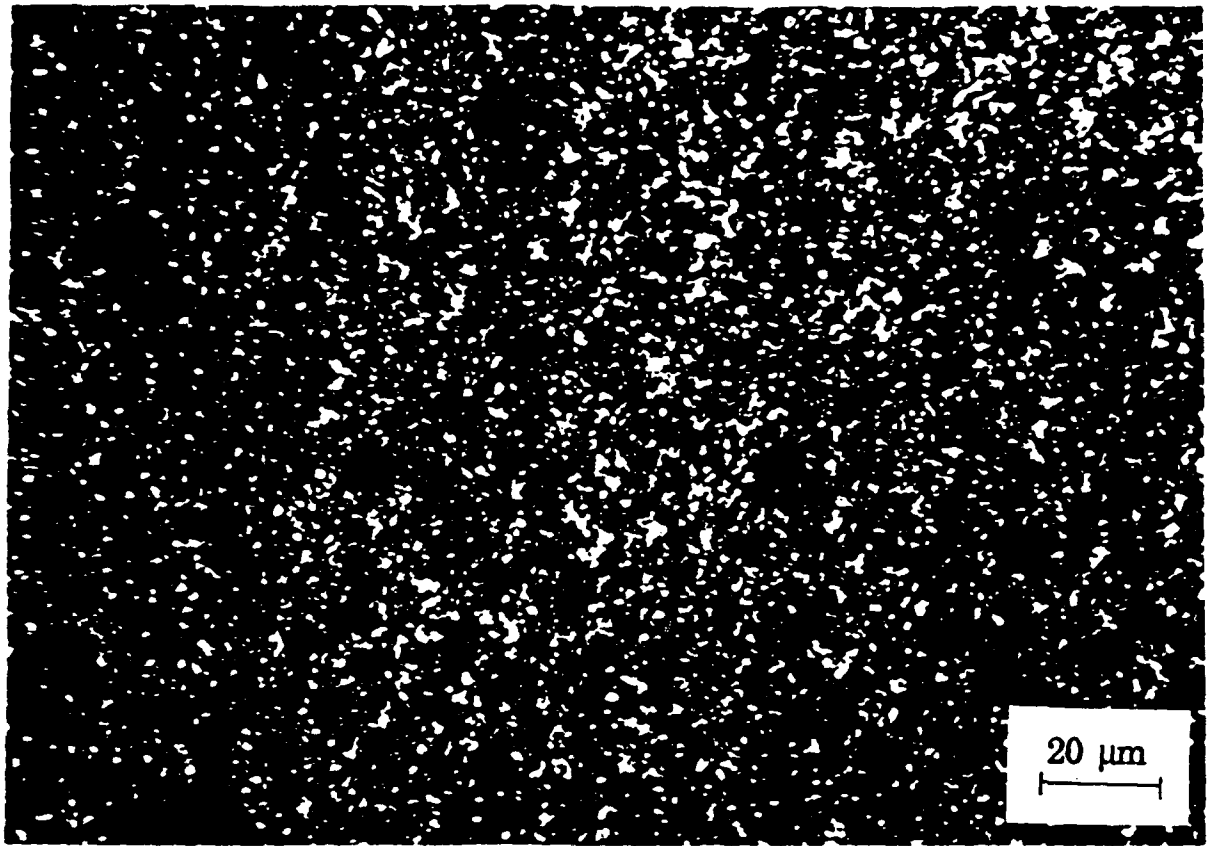
1. F.E.McFarlane, T.G.Davis; U.S. Patent 3890256 (1975).
2. Y. Ide, Z.Ophir; Poly. Eng. & Sci., 23,261 (1983).
3. Y. Ide, T.S.Chung; J. Macromol. Sci., Phys., B-23(4-6), 497 (1984-85).
4. G.W.Calundann, M. Jaffe; Anisotropic Polymers: Their Synthesis and Properties, in Proceedings of the Robert Welch Fdn. Conferences on Chemical Research XXVI. Synthetic Polymers, 247-291, (1982)
5. D.G.Baird, G.L.Wilkes; Poly. Eng. & Sci., 23, 633, (1983).
6. Z. Zhou, X. Wu, M.Wang; Poly. Eng. & Sci., 28, No. 3, 136, Feb.(1988).
7. P.G. Martin, S.I.Stupp; The Contrasting Behavior of Chemically Ordered vs. Chemically Disordered Liquid Crystal Polymers, Polymer Group Report #252, Univ. of Illinois, (1987).
8. S.I. Stupp, J.S. Moore, P.G. Martin; Chemical Disorder and Phase Separation: A Study of Two Liquid Crystal Polymers, Polymer Group Report #253, Univ. of Illinois, (1987).
9. C. Noel; Identification of Mesophases Exhibited by Liquid Thermotropic Liquid Crystalline Polymers, in Polymer Liquid Crystals, A. Blumstein, Editor, pp 21-63, Polymer Science and Technology Series Vol. 28, Plenum Press, N.Y. (1985).
10. L.C. Sawyer, M. Jaffe; J. Materials Science, 21, 1897-1913, (1986).
11. I.M.Ward; Proceedings Phys. Soc., 80, 1176, (1962).
12. G.R. Davies, I.M. Ward; Structure and Properties of Oriented

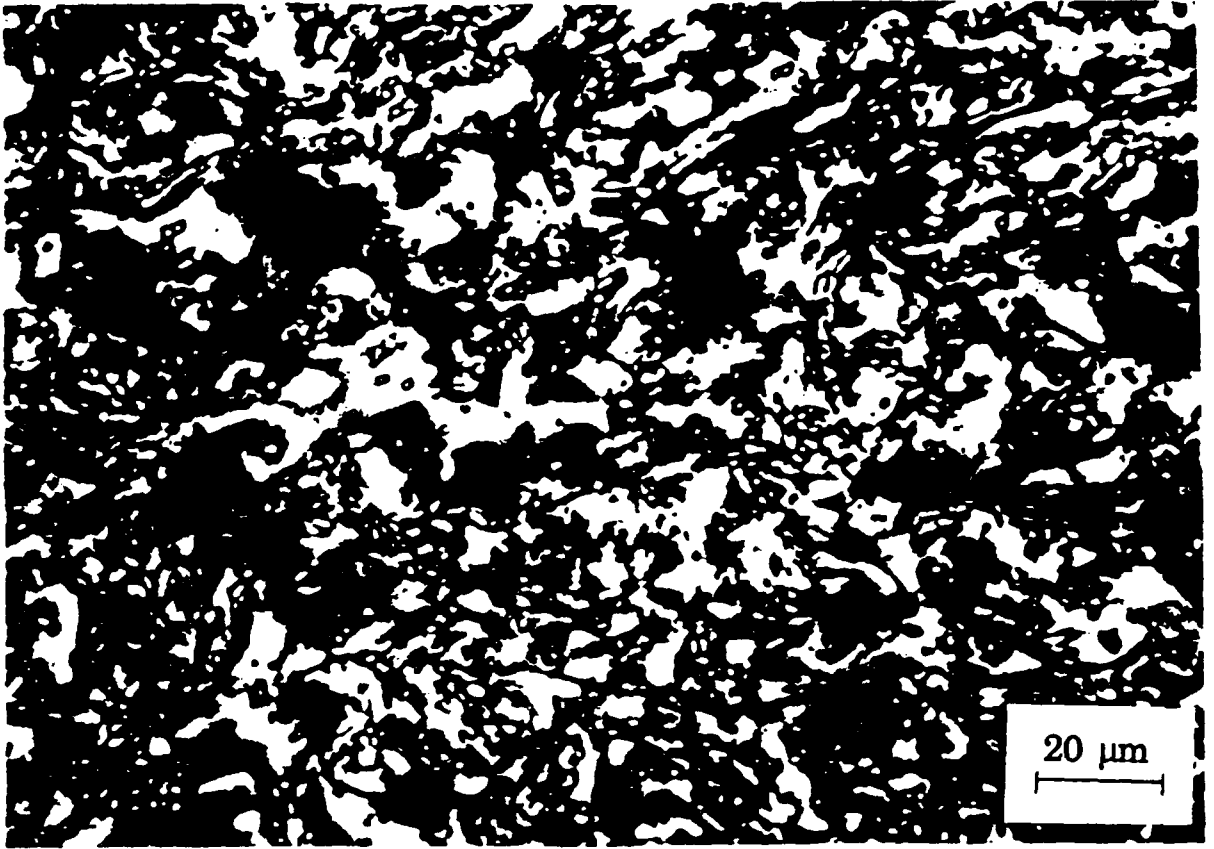
Thermotropic Liquid Crystalline Polymers in the Solid State,
Unpublished Review Article (1988).

- 13 L. Nicolais, L. Nicodemo, P. Masi, A.T. DiBenedetto; Poly. Eng. & Sci.,
19, No. 14, 1046, Nov. (1979).
14. J.E. Aston, J.C. Halpin, P.H. Petit; Primer on Composite Materials:
Analysis, pp 77-85, Technomics Pub. Co., Connecticut (1969).
15. J.K. Lees; Polymer Eng. and Sci., 8, 186, (1968).
16. L. Mandelkern; J. App. Phys., 26, 443, (1955).
17. M. Avrami; J. Chem. Phys., 7, 1103, (1939); 8, 212, (1940);
9, 177, (1941).

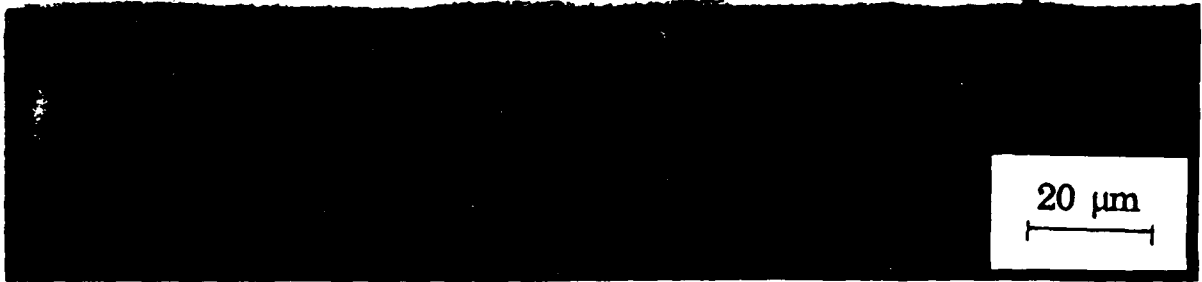
LIST OF FIGURES

1. Nematic domain structure of an unoriented film of PET/PHB60 as seen under cross polars. (a) 200°C for 10 min. (b) 260°C for 25 min. (c) 300°C for 10 min.
2. Drawn fibers of PET/PHB60 (DR=250) as seen under cross polars; (a) fiber axis at 45° with respect to the polars (b) fiber axis aligned with the polars
3. Fracture surfaces of PET/PHB60 drawn fibers, (a) Scanning electron micrograph (DR=300). (b) Optical micrograph with cross polars (DR=250)
4. Annealed LCP fibers (initial DR=250) as seen under cross polars. (a) Recoiled fiber at 230°C for 15 min. (b) Recoiled fiber at 270°C for 1 min.
5. Model of the LCP as it is being hot drawn. S_N = order parameter for the nematic domains. S_F = order parameter for the fiber. l/d = aspect ratio of the nematic domains during hot drawing.
6. Composite model for the oriented thermotropic material.
 $(E_L)_F$ = Longitudinal elastic modulus of the fiber
 $(E_T)_F$ = Transverse elastic modulus of the fiber.
 S_A = Order parameter for the phase boundaries
 X_N = Volume fraction of nematic domains.
7. Model for the rigid rod rotation of nematic domains during hot drawing.
8. Effect of draw ratio on the longitudinal elastic modulus of PET/PHB60 fibers. \square Experimental values; — Theoretical.
9. Shrinkage of drawn LCP fibers (DR=60) as a function of time and temperature. Δ 180°C; \circ 200°C; \square 220°C; ∇ 230°C; \diamond 240°C.
 $X(\infty)$ = maximum volume fraction transformed to nematic domains during annealing.
10. Shrinkage of drawn LCP fibers as a function of time at 240°C and DR=25 (∇) and DR=60 (\diamond); — Calculated for DR=60.
11. Correlation of shrinkage with volume fraction of transformed material DR=60; \circ Experimental temperatures vs. X ; — Theoretical shrinkage vs. transformed volume fraction.
12. The DSC spectrum for unprocessed PET/PHB60. Scanning rate = 10°C/min.



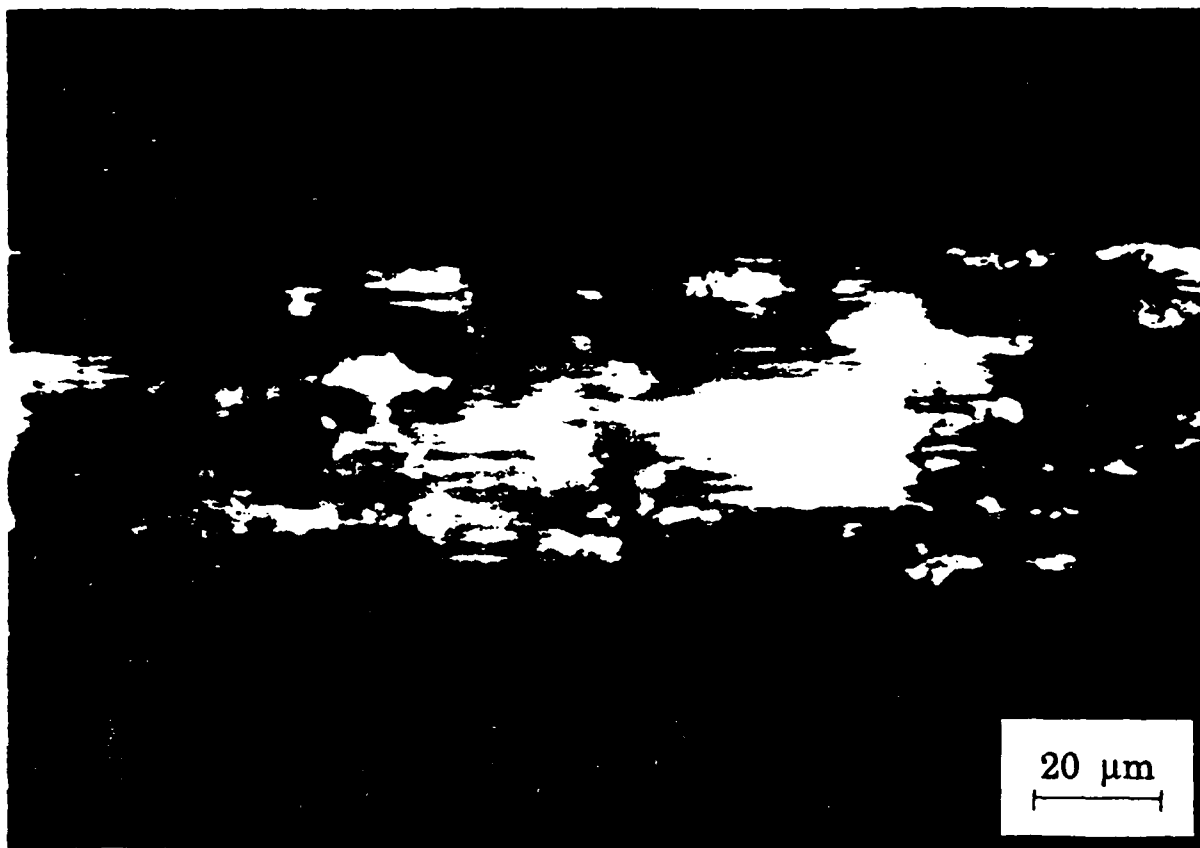




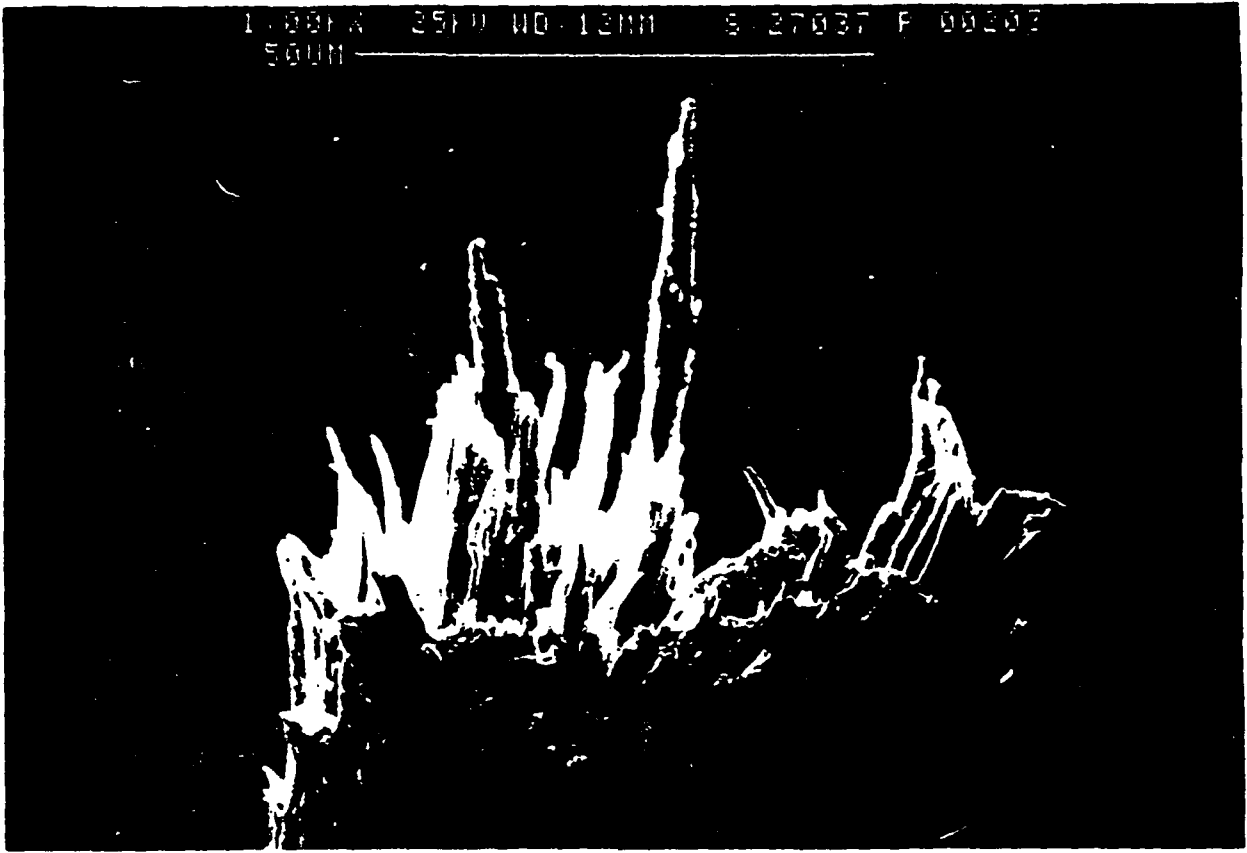


20 μm



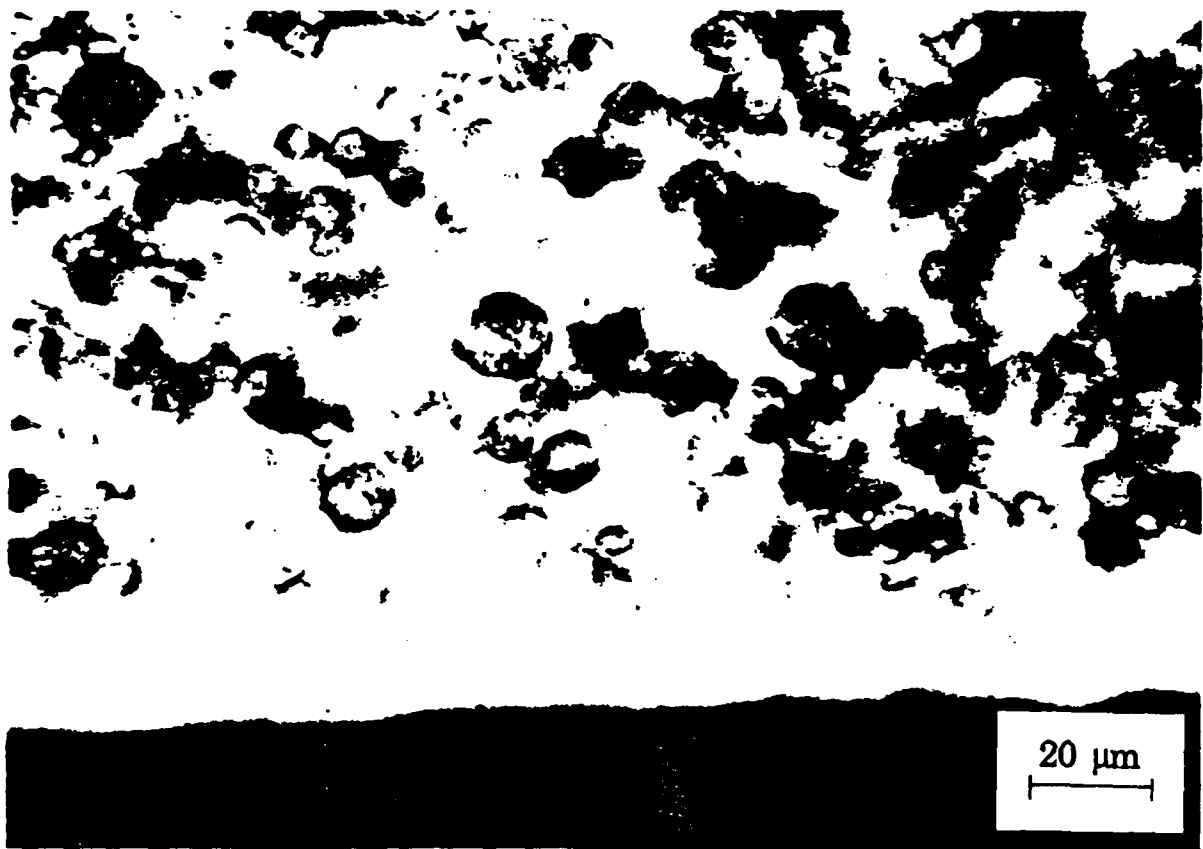


1.000A 25FD NO. 12MM S. 27037 P. 00202
50UM





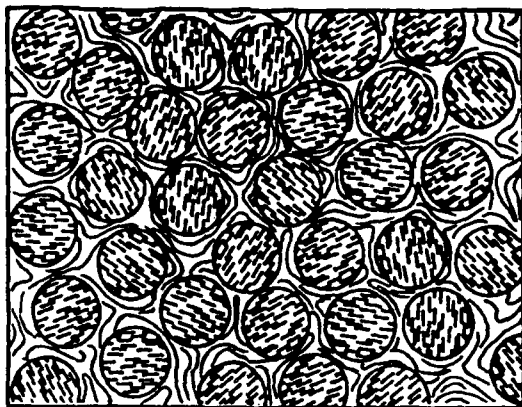




ORIENTATION OF THERMOTROPIC MATERIAL

$$S_N = S_F = 0$$

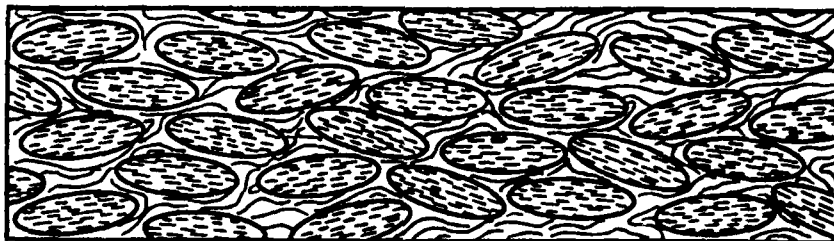
$$L/d \approx 1$$



$$0 < S_N < 1$$

$$0 < S_F < 1$$

$$1 < L/d < \infty$$

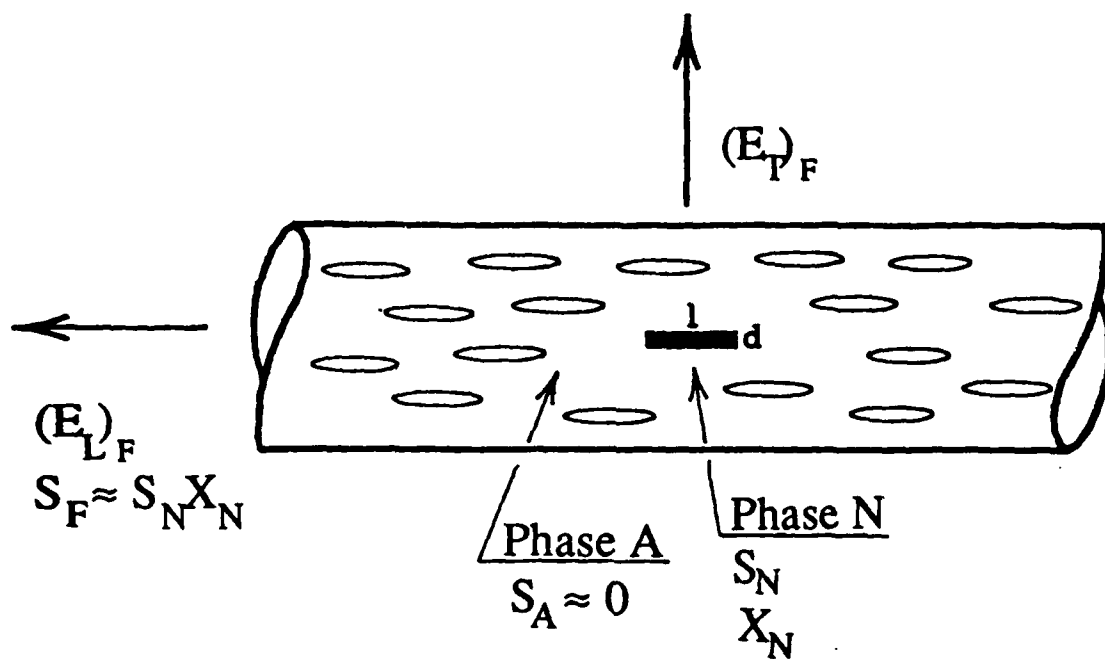


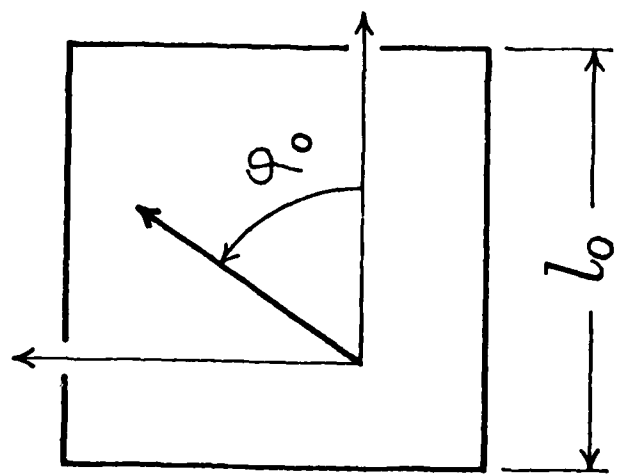
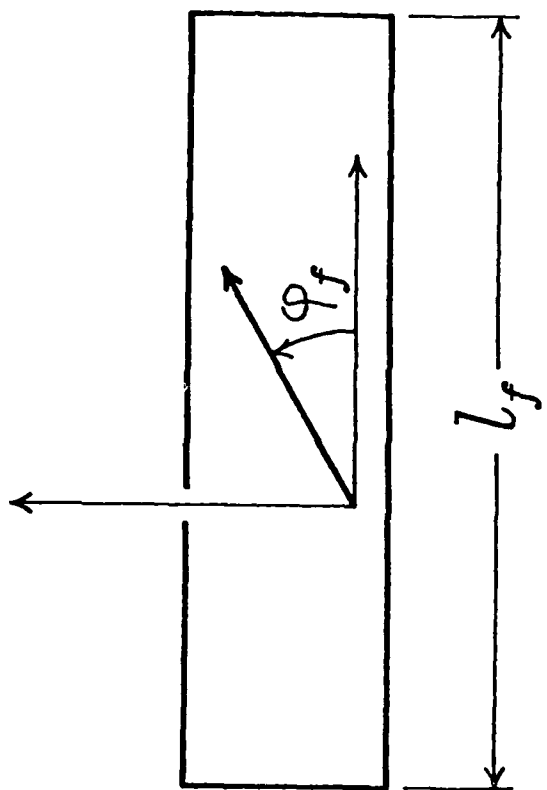
$$S_N = S_F \approx 1$$

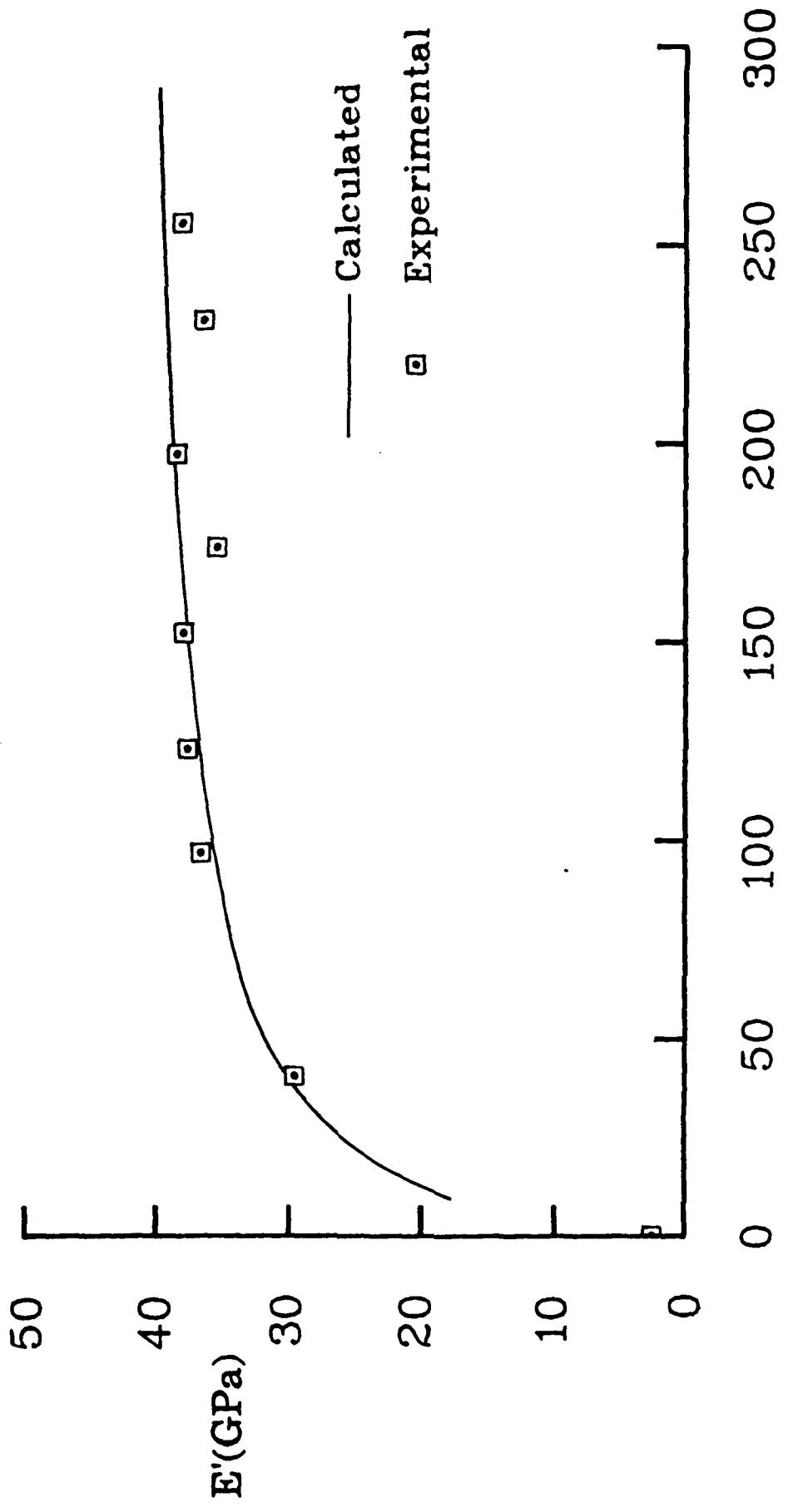
$$L/d = \infty$$



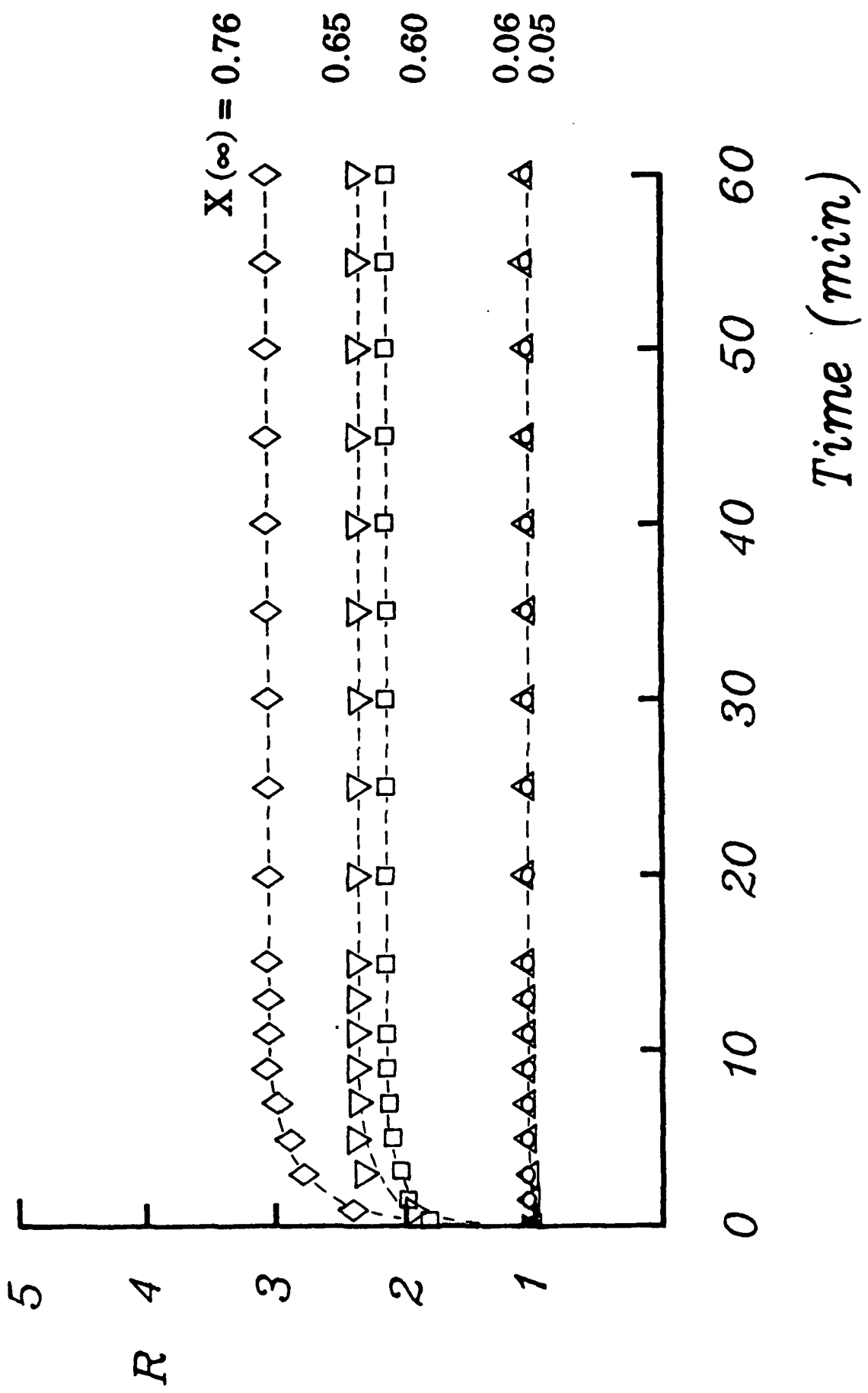
MODEL FOR ORIENTED THERMOTROPIC MATERIAL

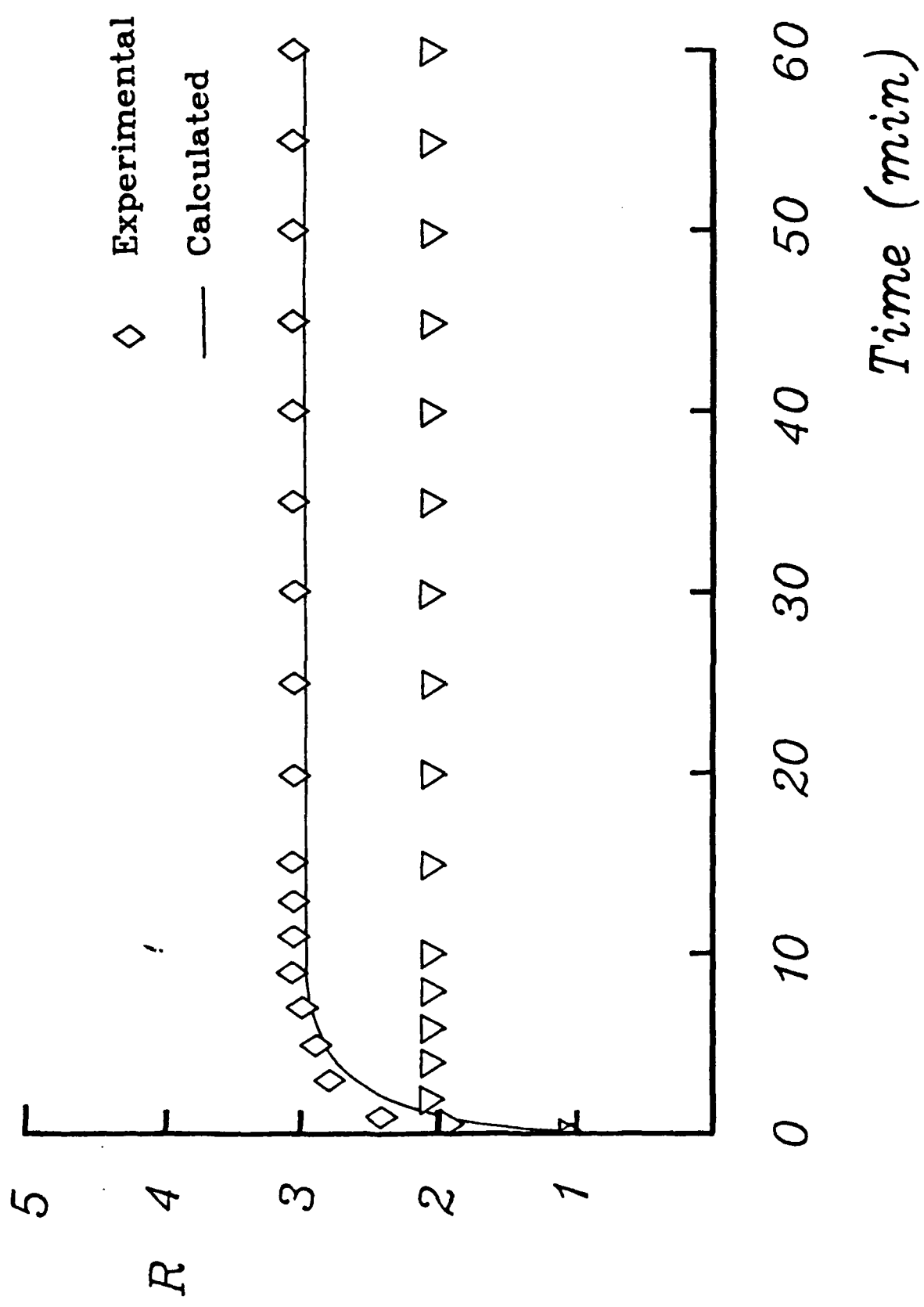


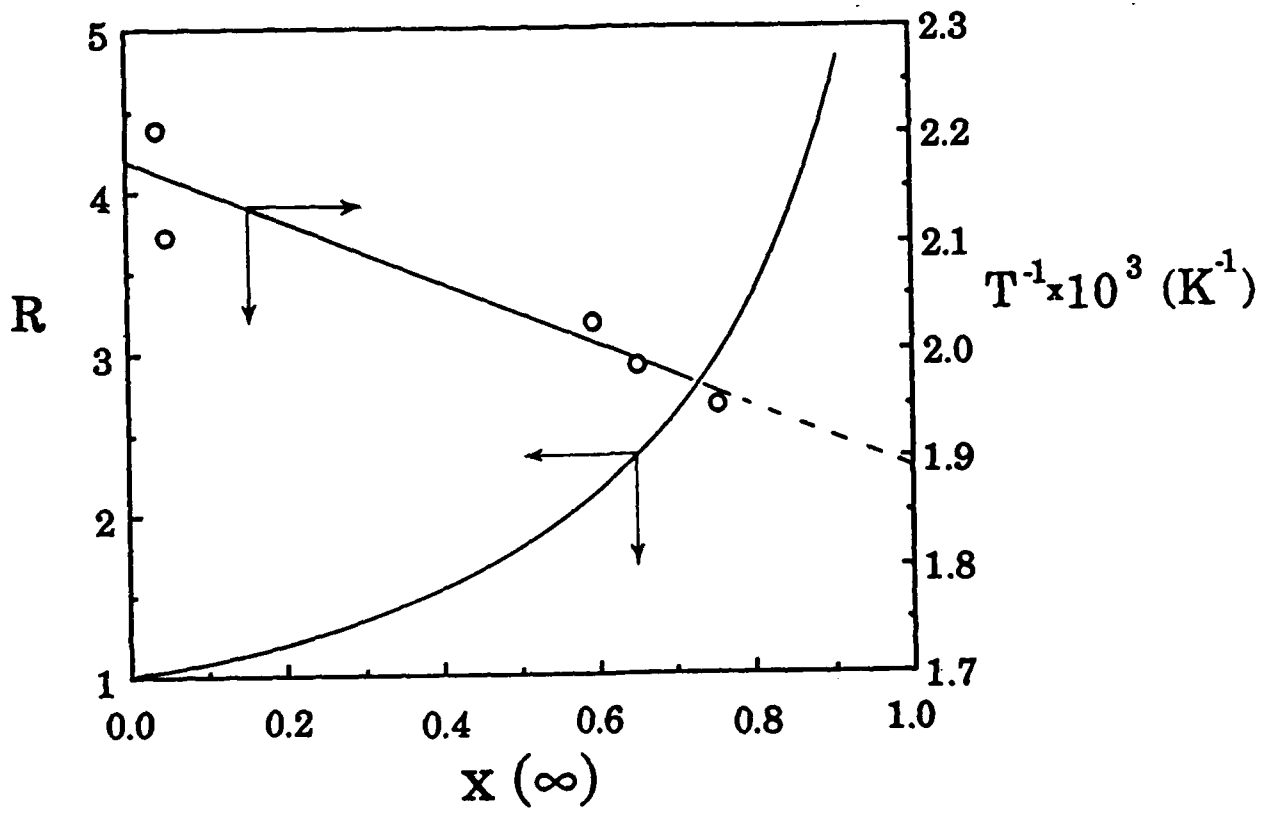


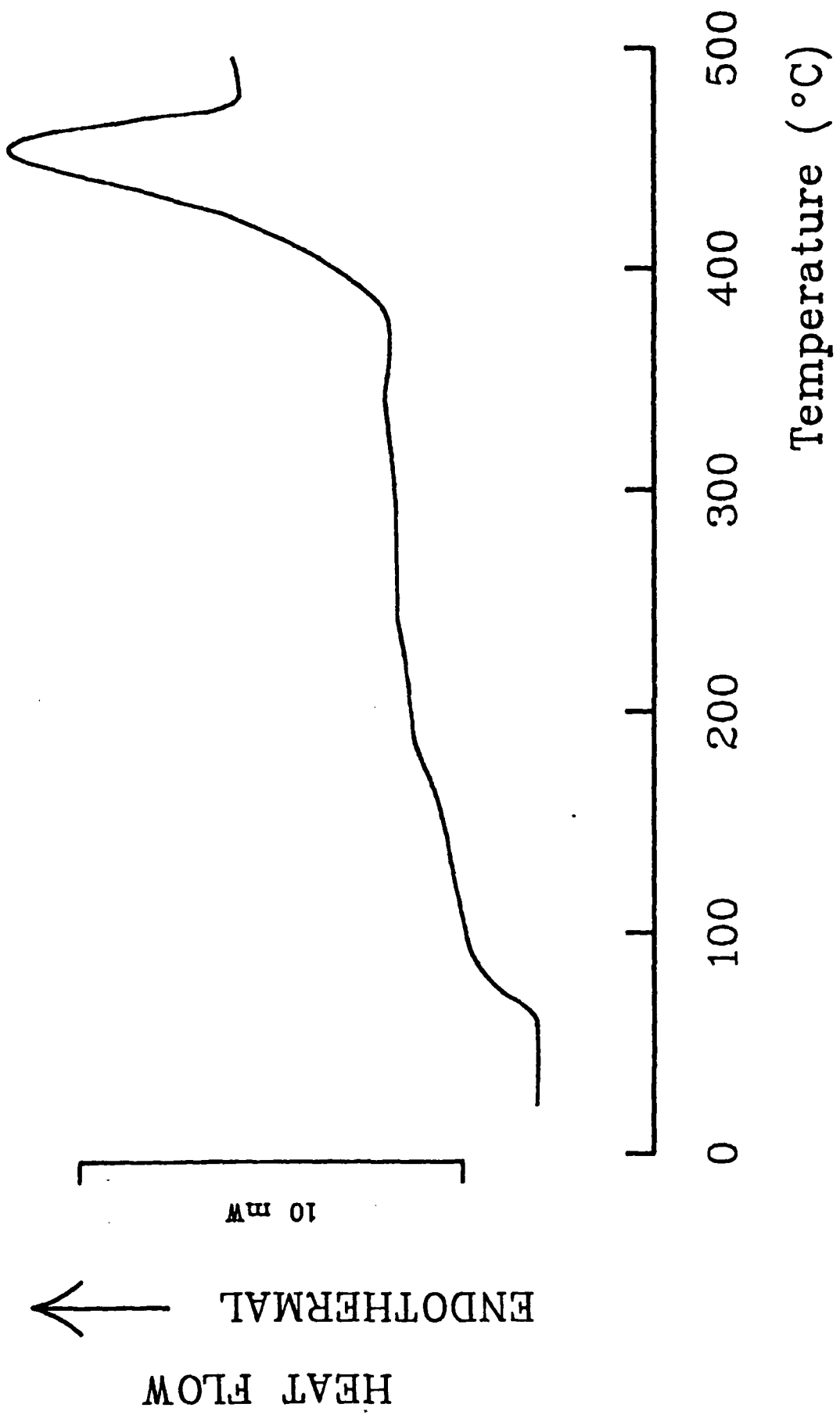


$$DR = S_o / S_f$$









TECHNICAL REPORT DISTRIBUTION LIST, GEN

| | <u>No. Copies</u> | | <u>No. Copies</u> |
|---|-----------------------|--|-----------------------|
| Office of Naval Research Attn: Code 1113 800 N. Quincy Street Arlington, Virginia 22217-5000 | 2 | Dr. David Young Code 334 NORDA NSTL, Mississippi 39529 | 1 |
| Dr. Bernard Duda Naval Weapons Support Center Code 50C Crane, Indiana 47522-5050 | 1 | Naval Weapons Center Attn: Dr. Ron Atkins Chemistry Division China Lake, California 93555 | 1 |
| Naval Civil Engineering Laboratory Attn: Dr. R. W. Drisko, Code LS2 Port Hueneme, California 93401 | 1 | Scientific Advisor Commandant of the Marine Corps Code RD-1 Washington, D.C. 20380 | 1 |
| Defense Technical Information Center Building 5, Cameron Station Alexandria, Virginia 22314 | 12 high quality | U.S. Army Research Office Attn: CRD-AA-IP P.O. Box 12211 Research Triangle Park, NC 27709 | 1 |
| DTNSRDC Attn: Dr. H. Singerman Applied Chemistry Division Annapolis, Maryland 21401 | 1 | Mr. John Boyle Materials Branch Naval Ship Engineering Center Philadelphia, Pennsylvania 19112 | 1 |
| Dr. William Tolles Superintendent Chemistry Division, Code 6100 Naval Research Laboratory Washington, D.C. 20375-5000 | 1 | Naval Ocean Systems Center Attn: Dr. S. Yamamoto Marine Sciences Division San Diego, California 91232 | 1 |